A study on cooperative navigation of AUVs based on bearing measurements

Pedro Mendes and Pedro Batista

Abstract— **In this work, two cooperative navigation solutions based on the extended Kalman filter are described. One of these is a centralized solution and the other is fully decentralized, taking full advantage of the benefits that come with decentralization, such as scalability and robustness. Simulations are performed for a formation of autonomous underwater vehicles with a fixed measurement topology. The vehicles are assumed to be equipped with sensors that allow them to take measurements of their depth and bearing angles to their neighbors. Two different topologies are considered, one acyclical and one cyclical. The transient and steady-state errors of both solutions are analyzed resorting to Monte Carlo simulations. In particular, the mean error and the root-mean-squared-error (RMSE) of the navigation estimates is presented.**

I. INTRODUCTION

There has been increasing interest in the development of robust autonomous underwater vehicle (AUV) systems for quite some time. In many commercial, scientific, and military applications, AUVs present many advantages over their manned counterpart. Some of these applications include scientific exploration, resource prospecting, archaeological surveying and salvaging, oceanographic mapping, and plenty of military applications, such as payload delivery, surveillance and mine termination, which are, by nature, repetitive or dangerous and thus more suitable for machines rather than people.

In order to develop reliable AUV systems, regardless of the mission at hand, a good navigation architecture is necessary, so that the control problem, which is more mission specific, can be independently tackled as well. In fact, most of the control algorithms rely on relatively good localization performance of the agents participating in the mission. However, in underwater applications, due to the attenuation of the conventional electromagnetic spectrum used for wireless communication, satellite-based navigation systems such as the GPS are unavailable. As such, different solutions based on relative measurements and communication between agents must be considered.

This work was supported by the Fundação para a Ciência e a Tecnologia (FCT) through LARSyS - FCT Project UIDB/50009/2020 and through the FCT project DECENTER [LISBOA-01-0145-FEDER-029605], funded by the Programa Operacional Regional de Lisboa 2020 and PIDDAC programs. This work has received funding from the European Union's Horizon 2020 research and innovation programme under grant agreement No. 101017808 (RAMONES project).

The authors are with the Institute for Systems and Robotics, LARSyS, Instituto Superior Técnico, Universidade de Lisboa, Portugal.

Emails: pedro.a.mendes@tecnico.ulisboa.pt pbatista@isr.tecnico.ulisboa.pt

Since centralized approaches often become impractical due to communication restrictions, there is a need for decentralized alternatives, in which AUVs only communicate locally and when necessary. These solutions are usually cooperative, that is, the AUVs communicate between themselves and work together to improve their estimates. Many of these cooperative techniques are based on Kalman filtering approaches, using the correlation of the agents in the formation as a way to achieve the desired cooperative behavior. The issue with this approach is that it becomes essential to keep track of the cross-correlation between agents, otherwise the Kalman filter may diverge [1], which is one of the main difficulties in achieving a decentralized cooperative localization solution of this type.

In this work, a general centralized approach to the problem of cooperative navigation of AUVs based on the extended Kalman filter (EKF) will be presented. Moreover, the decentralized version proposed in [2] will also be evaluated against it. Finally, the effect of the communication topology of the agents will also be studied, investigating whether the presence of cycles, with additional information, is beneficial to the performance of the whole system.

A. Related work

Early work that attempted to develop decentralized navigation solutions based on Kalman filtering techniques did so by reproducing the centralized solution at each vehicle, relying on communication schemes between the AUVs to distribute all the necessary data to each agent, such as in [3]. The proposed solution consists of having vehicles propagate their dead reckoning and measurement information to other AUVs through communication, and then having each agent carry a Kalman filter that estimates the position of the whole formation. While this approach is cooperative, by attempting to mimic the behavior of the centralized Kalman filter, it ends up requiring too much communication and does not take advantage of the scaling capabilities of decentralized solutions.

Some other early work on decentralized cooperative localization relied on bookkeeping strategies at each agent in order to correctly estimate the cross-covariances between AUVs. In [4], each agent maintains a set of filters, one for each possible combination of measurements between agents. Upon receiving a broadcast by its neighbors, each agent updates its compatible filters with the received information and then finds which filter among the ones in its database provides the best estimate.

978-0-692-93559-0 ©2021 MTS

Rather than attempting to build a centralized-equivalent estimator, which either requires excessive communication or complex bookkeeping strategies, some decentralized approaches instead attempt to approximate the centralized Kalman estimator. As mentioned before, the main issue with this kind of approach is the need for keeping track of the cross-correlation terms between each local filter.

In [5], the authors present a decentralized solution based on the covariance intersection algorithm to build a consistent Kalman filter estimator, guaranteeing that its estimates do not become overconfident. However, these estimates may also be overly pessimistic, as stated in [2]. Due to the decentralized nature of the proposed approach, the communication and processing requirements scale linearly with the number of neighboring AUVs at each agent, showing good scaling capabilities.

While this work is focused on Kalman filtering approaches, several other solutions have been proposed in the literature, including other probabilistic based techniques, such as particle filtering solutions, see e.g. [6] and [7]. Other approaches are based on writing globally convergent Kalman observers with linear-time varying dynamics and restricting the formation topology to guarantee global convergence to the solution, such as in [8]. Finally, some iterative optimization techniques for cooperative localization using range measurements have also been suggested, see e.g. [9].

B. Notation

For clarity purposes, the notation used in this work is defined here. Vectors $\mathbf{x} \in \mathbb{R}^n$ and matrices $\mathbf{A} \in \mathbb{R}^{m \times n}$ are represented using bold symbols, in lower and upper case, respectively. The i^{th} coordinate of a vector $\mathbf{p}$ is denoted as $\mathbf{p}^i$. The identity matrix is written as $\mathbf{I}_n \in \mathbb{R}^{n \times n}$ and a zero matrix as $\mathbf{0}_n \in \mathbb{R}^{n \times n}$. If the zero matrix is not square, it is represented as $\mathbf{0}_{m \times n}$. Additionally the transpose of a matrix $\mathbf{A}$ is written as $\mathbf{A}^T$, the diagonal operator is represented as $\text{diag}(\cdot)$, and $||\mathbf{x}||$ is the standard Euclidean norm of the vector $\mathbf{x}$.

II. Problem statement

Consider a set of AUVs, numbered from 1 to N, where each agent evolves according to

$$\begin{cases} \dot{\mathbf{p}}_i(t) = \mathbf{v}_{r_i}(t) + \mathbf{v}_{f_i}(t) \\ \dot{\mathbf{v}}_{f_i}(t) = \mathbf{0}_3 \end{cases}, \tag{1}$$

where $\mathbf{p}_i(t) \in \mathbb{R}^3$ represents the AUV's position in a local inertial frame $\{I\}$, $\mathbf{v}_{r_i}(t) \in \mathbb{R}^3$ is its velocity relative to the fluid it is operating in, expressed in inertial coordinates, and $\mathbf{v}_{f_i}(t) \in \mathbb{R}^3$ is the velocity of the fluid in inertial coordinates, which can be different for each AUV, though it is assumed to be constant. This is a valid assumption locally as long as the AUVs do not move very fast. In practice, by appropriate tuning of the filter parameters, it is possible to track slowly time-varying quantities.

Some AUVs, called *leaders*, have direct access to measurements of their position, acquired via GPS, for example. The other agents, called *followers*, are assumed to be operating in a GPS-denied environment and, as such, must perform localization through measurements and communication with other agents. In the setting considered here, the AUVs are capable of measuring their own depth and are also able to take bearing measurements about their neighbors. As such, if at time t_k an AUV i takes a measurement about an agent j, this measurement is modeled as

$$\begin{cases} \theta(t_k) = \theta(\mathbf{p}_i(t_k), \mathbf{p}_j(t_k)) \\ \phi(t_k) = \phi(\mathbf{p}_i(t_k), \mathbf{p}_j(t_k)) \\ z(t_k) = \mathbf{p}_i^z(t_k) \end{cases},$$

where θ and ϕ are the bearing angles measured by AUV i and z is its depth. Whenever an AUV takes a measurement about one of its neighbors, it is also assumed that they are capable of communicating with each other.

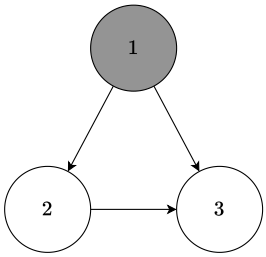

Fig. 1: Example communication graph $\mathcal{G}$.

The agents are assumed to travel through space with a fixed measurement configuration. Let $\mathcal{G} \coloneqq (\mathcal{V}, \mathcal{E})$ be the graph representing the measurement topology of the AUVs, such that $\mathcal{V} \coloneqq \{1, \ldots, N\}$ is the set of nodes in $\mathcal{G}$, representing agents 1 to N, and $\mathcal{E}$ is the set of edges in the graph. The edges represent information flow, that is, there is a directed edge $e = (i, j) \in \mathcal{E}$ from node i to node j if AUV j is capable of taking measurements about AUV i. Finally, denote the set of nodes that AUV i can take measurements about as the set of its neighbors, $\mathcal{N}_i$. An example of a measurement graph, $\mathcal{G}$, is represented in Fig. 1, where $\mathcal{V} = \{1, 2, 3\}$ and $\mathcal{E} = \{(1, 2), (1, 3), (2, 3)\}$. The leader, AUV 1, is represented in a shaded tone. The set of neighbors of AUV 3, in this example, is $\mathcal{N}_3 = \{1, 2\}$.

III. Centralized extended Kalman filter

In this section, a centralized extended Kalman filter (CEKF) for cooperative localization is presented. Besides assuming synchronicity between the measurements, in order to be implemented, this algorithm must rely on some kind of information distribution strategy. Either all agents have access to all the information that has been generated, such as dead-reckoning and measurement data, or some central unit must have access to this information and is then responsible for distributing the updated state estimates to all of the agents.

A. Motion model

The kinematic model (1) is continuous and therefore not suitable for direct use in the present navigation algorithm,

since bearing measurements are usually available at a slow rate. By discretizing it, one obtains

$$\begin{cases} \mathbf{p}_i(t_{k+1}) = \mathbf{p}_i(t_k) + T\mathbf{v}_{f_i}(t_k) + \mathbf{u}_i(k) \\ \mathbf{v}_{f_i}(t_{k+1}) = \mathbf{v}_{f_i}(t_k) \end{cases},$$

where

$$\mathbf{u}_i(k) \coloneqq \int_{t_k}^{t_{k+1}} \mathbf{v}_{r_i}(t)dt \tag{2}$$

and T is the sampling time. Defining the state of each agent as

$$\mathbf{x}_i(k) \coloneqq \begin{bmatrix} \mathbf{p}_i(t_k) \\ \mathbf{v}_{f_i}(t_k) \end{bmatrix},$$

the motion model for each AUV is given by

$$\mathbf{x}_i(k+1) = \mathbf{A}_i\mathbf{x}_i(k) + \mathbf{B}_i\mathbf{u}_i(k),$$

where

$$\mathbf{A}_i = \begin{bmatrix} \mathbf{I}_3 & T\mathbf{I}_3 \\ \mathbf{0}_3 & \mathbf{I}_3 \end{bmatrix} \qquad \text{and} \qquad \mathbf{B}_i = \begin{bmatrix} \mathbf{I}_3 \\ \mathbf{0}_3 \end{bmatrix}.$$

In order to design a centralized Kalman estimator, consider the state vector

$$\mathbf{x}(k) \coloneqq \begin{bmatrix} \mathbf{x}_1(k) \\ \vdots \\ \mathbf{x}_N(k) \end{bmatrix},$$

from which the centralized motion model is obtained as

$$\mathbf{x}(k+1) = \mathbf{A}\mathbf{x}(k) + \mathbf{B}\mathbf{u}(k),$$

where $\mathbf{A} = \operatorname{diag}(\mathbf{A}_1, \ldots, \mathbf{A}_N)$, $\mathbf{B} = \operatorname{diag}(\mathbf{B}_1, \ldots, \mathbf{B}_N)$, and $\mathbf{u} \coloneqq \begin{bmatrix} \mathbf{u}_1^T(k) & \cdots & \mathbf{u}_N^T(k) \end{bmatrix}^T$.

B. Observation model

For the sake of conciseness, the explicit time dependence of the measurement and state vectors is dropped from here onward when not necessary. Let i be the index of a leader AUV, which has direct access to measurements of its position, such that $\mathbf{y}_i \coloneqq \mathbf{p}_i(t_k)$, where $\mathbf{y}_i$ is the measurement vector. The observation model for agent i, with respect to the whole formation, is then given by

$$\mathbf{h}_i(\mathbf{x}) = \mathbf{J}_i\mathbf{x},$$

with $\mathbf{J}_i = \begin{bmatrix} \cdots & \mathbf{I}_3 & \mathbf{0}_3 & \cdots \end{bmatrix}$, where $\mathbf{I}_3$ occupies the columns corresponding to the position of the measuring agent in the complete state vector.

If, on the other hand, i is the index of a follower AUV, its measurements, apart from depth, will be about other agents. Denoting the AUVs that participate in a measurement as *participating* agents and the AUVs that do not as *non-participating* agents, the bearing measurement vector of the measuring AUV with index i, to another AUV with index j, can be written as a function of the state of participating AUVs as

$$\mathbf{y}_b = \mathbf{h}_b(\mathbf{x}_i, \mathbf{x}_j)|_{t=t_k},$$

where $\mathbf{h}_b(\mathbf{x}_i, \mathbf{x}_j) = \begin{bmatrix} \theta(\mathbf{x}_i, \mathbf{x}_j) & \phi(\mathbf{x}_i, \mathbf{x}_j) \end{bmatrix}^T$, and

$$\begin{cases} \theta(\mathbf{x}_i, \mathbf{x}_j) = \operatorname{atan2}\left(\mathbf{p}_j^z - \mathbf{p}_i^z, L_{xy}\right) \\ \phi(\mathbf{x}_i, \mathbf{x}_j) = \operatorname{atan2}\left(\mathbf{p}_j^y - \mathbf{p}_i^y, \mathbf{p}_j^x - \mathbf{p}_i^x\right) \end{cases},$$

with $L_{xy} = \sqrt{(\mathbf{p}_j^x - \mathbf{p}_i^x)^2 + (\mathbf{p}_j^y - \mathbf{p}_i^y)^2}$. The Jacobian of this observation model with respect to the whole formation, denoted by $\mathbf{J}_b$, is given by

$$\begin{aligned} \mathbf{J}_b(\mathbf{x}) &= \begin{bmatrix} \ldots & \dfrac{\partial \mathbf{h}_b}{\partial \mathbf{x}_i}(\mathbf{x}_i, \mathbf{x}_j) & \ldots & \dfrac{\partial \mathbf{h}_b}{\partial \mathbf{x}_j}(\mathbf{x}_i, \mathbf{x}_j) & \ldots \end{bmatrix} \\ &= \begin{bmatrix} \cdots & \mathbf{J}_{b_i}(\mathbf{x}_i, \mathbf{x}_j) & \cdots & \mathbf{J}_{b_j}(\mathbf{x}_i, \mathbf{x}_j) & \cdots \end{bmatrix}, \end{aligned}$$

where the explicit expressions of $\mathbf{J}_{b_i}(\mathbf{x}_i, \mathbf{x}_j)$ and $\mathbf{J}_{b_j}(\mathbf{x}_i, \mathbf{x}_j)$ are omitted due to space limitations. Here, $\mathbf{J}_{b_i}$ occupies the columns which correspond to the state of the agent with index i and $\mathbf{J}_{b_j}$ those of the agent with index j. Since an AUV might take measurements about more than one agent and is also able to take depth measurements, each follower AUV's observation model, $\mathbf{h}_i$, is a concatenation of bearing measurements to other agents in its neighbor set and its depth measurement. Its Jacobian, $\mathbf{J}_i$, is similarly a concatenation of the individual measurement model Jacobians with respect to the whole formation. As an example, the measurement vector of AUV 3 in the measurement graph depicted in Fig. 1 is given by

$$\mathbf{y}_3 = \begin{bmatrix} \mathbf{h}_b(\mathbf{x}_3, \mathbf{x}_1) \\ \mathbf{h}_b(\mathbf{x}_3, \mathbf{x}_2) \\ z_3 \end{bmatrix},$$

where z_3 is the depth measurement captured by agent 3. Similarly, its jacobian is given by

$$\mathbf{J}_3 = \begin{bmatrix} \mathbf{J}_{b_1}(\mathbf{x}_3, \mathbf{x}_1) & \mathbf{0}_{2\times 6} & \mathbf{J}_{b_3}(\mathbf{x}_3, \mathbf{x}_1) \\ \mathbf{0}_{2\times 6} & \mathbf{J}_{b_2}(\mathbf{x}_3, \mathbf{x}_2) & \mathbf{J}_{b_3}(\mathbf{x}_3, \mathbf{x}_2) \\ \mathbf{0}_{1\times 6} & \mathbf{0}_{1\times 6} & \mathbf{C}_z \end{bmatrix},$$

where $\mathbf{C}_z = \begin{bmatrix} 0 & 0 & 1 & 0 & 0 & 0 \end{bmatrix}$.

Consider the complete measurement vector, given by a concatenation of all the individual AUV measurements,

$$\mathbf{y} \coloneqq \begin{bmatrix} \mathbf{y}_1 \\ \vdots \\ \mathbf{y}_N \end{bmatrix},$$

such that $\mathbf{y} = \mathbf{h}(\mathbf{x})$. Here, $\mathbf{h}(\mathbf{x})$ corresponds to the concatenation of the respective individual observation models of AUVs 1 to N,

$$\mathbf{h}(\mathbf{x}) \coloneqq \begin{bmatrix} \mathbf{h}_1(\mathbf{x}) \\ \vdots \\ \mathbf{h}_N(\mathbf{x}) \end{bmatrix},$$

where $\mathbf{h}_i(\mathbf{x})$ is the measurement model of AUV i with respect to all the agents in the formation. The centralized Jacobian is then given by

$$\mathbf{J}(\mathbf{x}) = \begin{bmatrix} \mathbf{J}_1(\mathbf{x}) \\ \vdots \\ \mathbf{J}_N(\mathbf{x}) \end{bmatrix}.$$

Let $\hat{\mathbf{x}}(k+1|k)$ and $\hat{\mathbf{x}}(k+1|k+1)$ be the estimates of $\mathbf{x}$ at time $k+1$, before and after the update step of the Kalman filter, respectively. Additionally, let $\mathbf{\Sigma}(k+1|k)$ and $\mathbf{\Sigma}(k+1|k+1)$ be the corresponding state covariance

estimates. The prediction step, which corresponds to the motion update equations, is given by

$$\begin{cases} \hat{\mathbf{x}}(k+1|k) = \mathbf{A}\hat{\mathbf{x}}(k|k) + \mathbf{B}\mathbf{u}(k) \\ \mathbf{\Sigma}(k+1|k) = \mathbf{A}\mathbf{\Sigma}(k|k)\mathbf{A}^T + \mathbf{Q} \end{cases},$$

where $\mathbf{A}$ and $\mathbf{B}$ were defined in the previous section and $\mathbf{Q}$ is the process noise covariance matrix, which can be defined for each AUV, and then concatenated as $\mathbf{Q} = \mathrm{diag}(\mathbf{Q}_1, \ldots, \mathbf{Q}_N)$. The update equations, to be performed upon receiving a measurement, are given by

$$\begin{cases} \hat{\mathbf{x}}(k+1|k+1) = \hat{\mathbf{x}}(k+1|k) + \mathbf{K}(\mathbf{y} - \hat{\mathbf{y}}) \\ \mathbf{\Sigma}(k+1|k+1) = \left(\mathbf{I}_{6N} - \mathbf{K}\hat{\mathbf{J}}\right)\mathbf{\Sigma}(k+1|k) \end{cases},$$

where $\hat{\mathbf{J}} = \mathbf{J}(\hat{\mathbf{x}}(k+1|k))$ is the Jacobian of the centralized measurement model evaluated at the current state estimate, $\mathbf{K} = \mathbf{\Sigma}(k+1|k)\hat{\mathbf{J}}^T\left(\hat{\mathbf{J}}\mathbf{\Sigma}(k+1|k)\hat{\mathbf{J}}^T + \mathbf{R}\right)^{-1}$ is the Kalman gain, $\hat{\mathbf{y}} = \mathbf{h}(\hat{\mathbf{x}}(k+1|k))$ is the filter's expected measurement vector, and $\mathbf{R}$ is the measurement noise covariance matrix, which can also be defined for each measurement independently, analogously to $\mathbf{Q}$.

IV. Decentralized extended Kalman filter

In this section, an implementation of the solution presented in [2] is described for depth and bearing measurements, which will be labeled in this work as the decentralized extended Kalman filter (DEKF). This asynchronous approach is completely decentralized and relies only on local communication between neighboring agents.

A. Motion model

The first insight behind this solution is that the cross-covariances between agents are only necessary when update steps happen. Because of this, if each agent can correctly update its cross-covariance to other agents without communicating with them, the prediction step of the Kalman filter presents no issue.

Let the state of agent i be defined and denoted as $\mathbf{x}_i(k) \coloneqq \begin{bmatrix}\mathbf{p}_i^T(t_k) & \mathbf{v}_{f_i}^T(t_k)\end{bmatrix}^T$, and denote its filtered estimate and covariance as $\hat{\mathbf{x}}_i$ and $\hat{\mathbf{\Sigma}}_{ii}$, respectively. Note that the DEKF approximates the CEKF, thus the covariances of each agent and their cross-covariances to other agents will not be exact, hence the chosen hat notation. Consider the decomposition of the cross-covariance between agents i and j, $\hat{\mathbf{\Sigma}}_{ij}$, such that

$$\hat{\mathbf{\Sigma}}_{ij}(k) = \hat{\mathbf{\Phi}}_{ij}(k)\hat{\mathbf{\Phi}}_{ji}^T(k),$$

and let each agent carry its estimated belief, $\mathcal{B}_i \coloneqq \{\hat{\mathbf{x}}_i, \hat{\mathbf{\Sigma}}_{ii}\}$, and cross-covariance factor, $\hat{\mathbf{\Phi}}_{ij}$, between itself and other agents it has knowledge of, i.e., each agent i carries $\mathcal{B}_i$ and $\hat{\mathbf{\Phi}}_{ij}$ for all $j \in \mathcal{N}_i$.

The corresponding CEKF prediction equations for agent i, which account for its motion, are given by

$$\begin{cases} \hat{\mathbf{x}}_i(k+1|k) = \mathbf{A}_i\hat{\mathbf{x}}_i(k|k) + \mathbf{B}_i\mathbf{u}_i(k) \\ \mathbf{\Sigma}_{ii}(k+1|k) = \mathbf{A}_i\mathbf{\Sigma}_{ii}(k|k)\mathbf{A}_i^T + \mathbf{Q}_i \\ \mathbf{\Sigma}_{ij}(k+1|k) = \mathbf{A}_i\mathbf{\Sigma}_{ij}(k|k) \end{cases}, \tag{3}$$

leaving the remaining terms $\hat{\mathbf{x}}_j, \mathbf{\Sigma}_{jj}, \forall j \neq i$, unchanged. So, if AUV i updates its cross-covariance factor to another AUV j through

$$\hat{\mathbf{\Phi}}_{ij}(k+1|k) = \mathbf{A}_i\hat{\mathbf{\Phi}}_{ij}(k|k) \ \forall j \neq i \tag{4}$$

when performing prediction steps, when they meet, their reconstructed cross-covariance is given by

$$\begin{aligned} \hat{\mathbf{\Sigma}}_{ij}(k+1|k) &= \mathbf{A}_i\hat{\mathbf{\Phi}}_{ij}(k|k)\hat{\mathbf{\Phi}}_{ji}(k|k)^T \\ &= \mathbf{A}_i\hat{\mathbf{\Sigma}}_{ij}(k|k) \\ &= \mathbf{\Sigma}_{ij}(k+1|k), \end{aligned}$$

if it holds that $\hat{\mathbf{\Sigma}}_{ij}(k|k) = \mathbf{\Sigma}_{ij}(k|k)$. In general, one has $\hat{\mathbf{\Sigma}}_{ij}(k|k) \neq \mathbf{\Sigma}_{ij}(k|k)$ due to approximations in the update step, however, what is important is that, since all terms are available, the prediction step of the CEKF can be reproduced exactly at each agent in a decentralized way without communication, thus resulting in no loss of estimation capabilities with respect to this step. All AUVs then predict their beliefs and cross-covariance factors to other agents according to (3) and (4), substituting their estimated belief by $\hat{\mathbf{x}}_i$ and $\mathbf{\Sigma}_{ii}$.

B. Observation model

A major difference should now be noted between the centralized and decentralized versions of this filter. While all the measurements are available simultaneously for computation of the update step in the CEKF, the DEKF is asynchronous and, as such, only one measurement vector is considered at a time. In a centralized approach, this would be equivalent to considering an observation model containing only one measurement at a time and performing several updates at each time step. Due to space limitations, the derivation of the update equations for measurements taken by the agents is not presented here, though they originate from the decomposition of the CEKF update equations, similarly to what was done in the previous section. The derivation of the update equations can be found in the appendix of the original work [2].

Consider that a leader AUV with index i takes a measurement of its position $\mathbf{y}_i$. Again, dropping the explicit time dependence, the measurement model for this agent is given by

$$\mathbf{h}(\mathbf{x}_i) = \begin{bmatrix}\mathbf{I}_3 & \mathbf{0}_3\end{bmatrix}\mathbf{x}_i = \mathbf{C}_i\mathbf{x}_i.$$

Since this equation only involves the measuring agent, the estimated belief and cross-covariance factors to other agents are updated according to

$$\begin{cases} \hat{\mathbf{x}}_i(k+1|k+1) = \hat{\mathbf{x}}_i(k+1|k) + \mathbf{K}_i(\mathbf{y}_i - \hat{\mathbf{y}}_i) \\ \hat{\mathbf{\Sigma}}_{ii}(k+1|k+1) = \left(\mathbf{I}_6 - \mathbf{K}_i\mathbf{C}_i\right)\hat{\mathbf{\Sigma}}_{ii}(k+1|k) \\ \hat{\mathbf{\Phi}}_{ij}(k+1|k+1) = \left(\mathbf{I}_6 - \mathbf{K}_i\mathbf{C}_i\right)\hat{\mathbf{\Phi}}_{ij}(k+1|k) \end{cases}, \tag{5}$$

where $\hat{\mathbf{y}}_i = \mathbf{h}(\hat{\mathbf{x}}_i)$ is the expected measurement vector, $\mathbf{K}_i$ is the Kalman gain, given by

$$\mathbf{K}_i = \hat{\mathbf{\Sigma}}_{ii}(k+1|k)\mathbf{C}_i^T\left(\mathbf{C}_i\hat{\mathbf{\Sigma}}_{ii}(k+1|k)\mathbf{C}_i^T + \mathbf{R}_i\right)^{-1},$$

and $\mathbf{R}_i$ is the measurement noise covariance matrix. Note that the last equation of (5) should be performed for all

agents that AUV i has knowledge of. In a centralized Kalman filter, measurements taken by an agent also affect the state of all agents that are correlated with it through previous measurements. However, in order to prevent excessive communication, the estimated beliefs of other agents are left unchanged.

If, instead, it is the case that a follower AUV i takes a bearing measurement about another AUV j and a depth measurement about itself then, letting $\hat{\mathbf{x}}_a$ be the joint estimate of the states $\mathbf{x}_i$ and $\mathbf{x}_j$, and $\hat{\mathbf{\Sigma}}_{aa}$ its estimated covariance, such that

$$\hat{\mathbf{x}}_a \coloneqq \begin{bmatrix} \hat{\mathbf{x}}_i \\ \hat{\mathbf{x}}_j \end{bmatrix} \qquad \text{and} \qquad \hat{\mathbf{\Sigma}}_{aa} \coloneqq \begin{bmatrix} \hat{\mathbf{\Sigma}}_{ii} & \hat{\mathbf{\Sigma}}_{ij} \\ \hat{\mathbf{\Sigma}}_{ji} & \hat{\mathbf{\Sigma}}_{jj} \end{bmatrix}.$$

Then, the update equations for the joint system are given by

$$\begin{cases} \hat{\mathbf{x}}_a(k+1|k+1) = \hat{\mathbf{x}}_a(k+1|k) + \mathbf{K}_a(\mathbf{y}_i - \hat{\mathbf{y}}_i) \\ \hat{\mathbf{\Sigma}}_{aa}(k+1|k+1) = \left(\mathbf{I}_6 - \mathbf{K}_a\hat{\mathbf{J}}_a\right)\hat{\mathbf{\Sigma}}_{aa}(k+1|k) \end{cases}. \tag{6}$$

In the above, $\mathbf{y}_i$ is the concatenation of the bearing measurement to another AUV with the captured depth measurement, $\hat{\mathbf{y}}_i$ is its predicted value, $\hat{\mathbf{J}}_a = \begin{bmatrix} \mathbf{J}_{f_i}(\hat{\mathbf{x}}_i, \hat{\mathbf{x}}_j) & \mathbf{J}_{f_j}(\hat{\mathbf{x}}_i, \hat{\mathbf{x}}_j) \end{bmatrix}$ is the Jacobian matrix of the joint system's measurement model, evaluated at the current state estimate, with $\mathbf{J}_{f_i}$ and $\mathbf{J}_{f_j}$ defined such that

$$\mathbf{J}_{f_i}(\mathbf{x}_i, \mathbf{x}_j) \coloneqq \begin{bmatrix} \mathbf{J}_{b_i}(\mathbf{x}_i, \mathbf{x}_j) \\ \mathbf{e}_z \end{bmatrix},$$
$$\mathbf{J}_{f_j}(\mathbf{x}_i, \mathbf{x}_j) \coloneqq \begin{bmatrix} \mathbf{J}_{b_j}(\mathbf{x}_i, \mathbf{x}_j) \\ \mathbf{0}_{1\times 3} \end{bmatrix},$$

where $\mathbf{e}_z \coloneqq \begin{bmatrix} 0 & 0 & 1 \end{bmatrix}$ and $\mathbf{K}_a$ is the Kalman gain, given by

$$\mathbf{K}_a = \hat{\mathbf{\Sigma}}_{aa}(k+1|k)\hat{\mathbf{J}}_a^T \left(\hat{\mathbf{J}}_a\hat{\mathbf{\Sigma}}_{aa}(k+1|k)\hat{\mathbf{J}}_a^T + \mathbf{R}_i\right)^{-1}.$$

These quantities can be computed locally at the measuring agent, requiring only that AUV j transmits its estimated belief, $\mathcal{B}_j$, and its cross-covariance factor to agent i, $\hat{\mathbf{\Phi}}_{ji}$. AUV i is then responsible for communicating to AUV j its updated belief, obtained from $\hat{\mathbf{x}}_a(k+1|k+1)$ and $\hat{\mathbf{\Sigma}}_{aa}(k+1|k+1)$. In order not to double count information, the cross-covariance between agents i and j must be distributed correctly. Since the decomposition of the cross-covariance between agents can be done in any way, it can be agreed beforehand that, upon receiving updated estimates, agent j sets its cross-covariance factor to AUV i as the identity matrix, i.e. $\hat{\mathbf{\Phi}}_{ji}(k+1|k+1) = \mathbf{I}_6$, and AUV i sets

$$\hat{\mathbf{\Phi}}_{ij}(k+1|k+1) = \hat{\mathbf{\Sigma}}_{ij}(k+1|k+1), \tag{7}$$

where $\hat{\mathbf{\Sigma}}_{ij}$ can be obtained from the updated joint state covariance matrix $\hat{\mathbf{\Sigma}}_{aa}$. This way, the cross-covariance between these two agents is preserved without need for communicating to agent j a new cross-covariance factor, since

$$\hat{\mathbf{\Phi}}_{ij}(k+1|k+1)\mathbf{I}_6^T = \hat{\mathbf{\Sigma}}_{ij}(k+1|k+1).$$

As before, in order to prevent communication between participating and non-participating agents, the state and covariance estimates of the latter are left unchanged.

The only terms that still need to tracked are the cross-covariance factors between participating and non-participating agents. This is the main contribution of the work in [2] and, as such, only the main result is presented here, though the interested reader can check the original work for details. The last update equation performed by participating agents is

$$\hat{\mathbf{\Phi}}_{il}(k+1|k+1) = \hat{\mathbf{\Sigma}}_{ii}(k+1|k+1)\hat{\mathbf{\Sigma}}_{ii}^{-1}(k+1|k)\hat{\mathbf{\Phi}}_{il}(k+1|k), \tag{8}$$

where i is the index of participating AUVs and l is the index of any non-participating AUV. Note that both participating agents should perform update (8).

To summarize, prediction steps are performed using the first two equations of (3) and (4); the correction updates performed by leader AUVs when they take a measurement of their position are given by (5); and when agent i takes a measurement about AUV j, these updates are done using (6), (7) and (8), with AUV j setting $\hat{\mathbf{\Phi}}_{ji}(k+1|k+1) = \mathbf{I}_6$ upon receiving its updated belief and performing (8) locally as well.

V. Simulation results

In this section, the simulation results of both approaches are presented. The algorithms are compared in two different settings, one where the measurement graph is acyclical, and one where there are cycles present in the graph, which provide additional information. A Monte Carlo analysis of each setting was performed, whereby 500 runs of a certain trajectory were simulated for each measurement topology. In order to better compare the algorithms, the i^{th} run of each setting was affected by the same initial state estimation errors and noise conditions.

A. Setup

The agents are assumed to be moving in a formation such that all AUVs follow the same trajectory, offset by their initial positions, detailed in Table I. Their trajectory relative to their initial position, $\mathbf{s}(t) = \mathbf{p}_i(t) - \mathbf{p}_i(0)$, is depicted in Fig. 2. The fluid velocity was set as constant throughout the whole operating space such that $\mathbf{v}_{f_i} = \begin{bmatrix} 0.1 & -0.2 & 0 \end{bmatrix}^T \mathrm{m/s}$ for all $i \in \mathcal{V}$, where $\mathcal{V}$ is the set of AUVs.

The leader AUVs are able to obtain position measurements corrupted by zero mean white Gaussian noise, with covariance matrix $\mathbf{\Sigma}_{\text{pos}} = \operatorname{diag}\left(0.3^2\mathbf{I}_2, 0.1^2\right)$. The depth measurements of the follower AUVs are corrupted by zero mean white Gaussian noise, with standard deviation of $0.2\,\mathrm{m}$, and the measured bearing angles, θ and ϕ, are corrupted by independent zero mean Gaussian noise, with standard deviation of $0.03\,\mathrm{rad}$. These are assumed to be available every $T = 2\,\mathrm{s}$, whereas the relative velocity of each agent, $\mathbf{v}_{r_i}$, is available at a rate of $50\,\mathrm{Hz}$ and is corrupted by zero mean white Gaussian noise, with covariance matrix $\mathbf{\Sigma}_u = 0.01^2\mathbf{I}_3$. The control signal of each agent, $\mathbf{u}_i(k)$, is obtained using the trapezoidal integration of $\mathbf{v}_{r_i}$ in between measurement time steps, approximating (2).

TABLE I: Initial positions of each AUV.

i	$\mathbf{p}_i^x(0)$ (m)	$\mathbf{p}_i^y(0)$ (m)	$\mathbf{p}_i^z(0)$ (m)
1	-50	-100	0
2	50	100	0
3	-110	-170	-190
4	-120	150	-210
5	100	-200	-230
6	120	190	-190
7	20	15	-350

As for the filter parameters, the states of each agent were considered to be completely uncorrelated at time $t = 0$, i.e., all cross-covariances, both in the CEKF and DEKF solutions, were set as the zero matrix, $\mathbf{0}_6$. Each agent's initial covariance matrix was set as $\hat{\mathbf{\Sigma}}_{ii}(0) = \text{diag}\left(20^2\mathbf{I}_3, 2^2\mathbf{I}_3\right)\ \forall i \in \mathcal{V}$. The process noise covariance matrix for each agent was set as $\mathbf{Q}_i = \text{diag}\left(0.1^2\mathbf{I}_3, 0.05^2\mathbf{I}_3\right)$. For the position measurements, the noise covariance matrix was set as $\mathbf{R}_i = \mathbf{I}_3$, whereas for the bearing measurements it was set as $\mathbf{R}_b = 0.05^2\mathbf{I}_2$, and for the depth measurements $\sigma_d = 0.3$ was considered. Finally, the initial estimate of each AUV was sampled from a Gaussian distribution, with mean identical to the true state of each AUV, and covariance matrix $\mathbf{\Sigma}_0 = \text{diag}(\mathbf{I}_3, 0.1^2\mathbf{I}_3)$ for leader AUVs, and $\mathbf{\Sigma}_0 = \text{diag}(15^2\mathbf{I}_3, 1^2\mathbf{I}_3)$ for follower AUVs. Note that, because the approaches are based on the EKF, global convergence properties are not guaranteed, and fine tuning of the filter parameters is required.

Both the CEKF and DEKF approaches were simulated considering two different topologies, differing from each other only in that one is acyclical and the other is not. The measurement graphs for each setting, $\mathcal{G}_1$ and $\mathcal{G}_2$, are presented in Figs. 3 and 4. A Monte Carlo analysis of $N = 500$ runs was made, whereby both algorithms were tested, in each topology, under the same noise conditions and initial state estimation errors in each run.

In order to evaluate the performance of the estimators, the root-mean-squared-error (RMSE) of the position and fluid velocity estimates, obtained for each time instant from the collection of Monte Carlo runs, was computed, such that

$$\text{RMSE}(\mathbf{x}(k)) = \sqrt{\frac{\sum_{n=1}^{N} ||\mathbf{x}(k) - \hat{\mathbf{x}}^n(k)||^2}{N}},$$

where $\mathbf{x}(k)$ is the concatenation of the position or fluid velocity vectors of all AUVs at time k, and $\hat{\mathbf{x}}^n(k)$ is its CEKF or DEKF estimate obtained in the n^{th} Monte Carlo run. Additionally, in order to investigate whether the estimators are biased, the mean error of the estimated quantities, for each time instant, was computed from the collection of Monte Carlo runs, as given by

$$\text{mean}(\mathbf{x}(k)) = \frac{1}{N}\sum_{n=1}^{N}\left(\mathbf{x}(k) - \hat{\mathbf{x}}^n(k)\right).$$

B. Sample run

For clarity purposes, only the results pertaining to AUVs 3, 4, and 7 are presented. Figs. 5 and 6 show the convergence

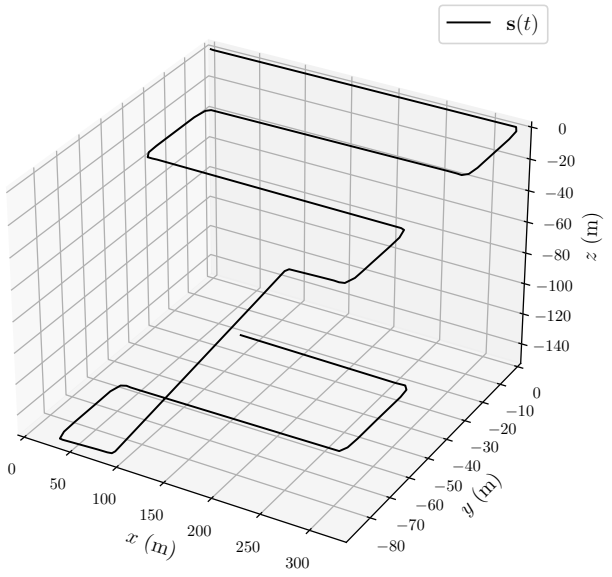

Fig. 2: Nominal trajectories of each AUV, translated so they start at the origin.

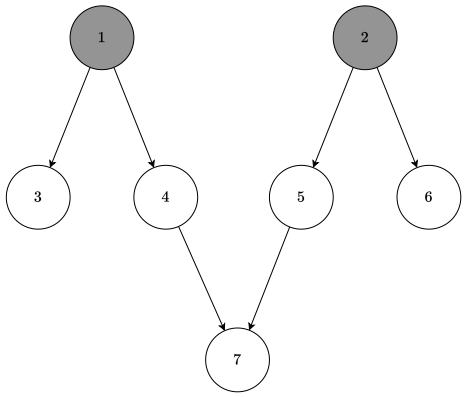

Fig. 3: Acyclical communication graph $\mathcal{G}_1$.

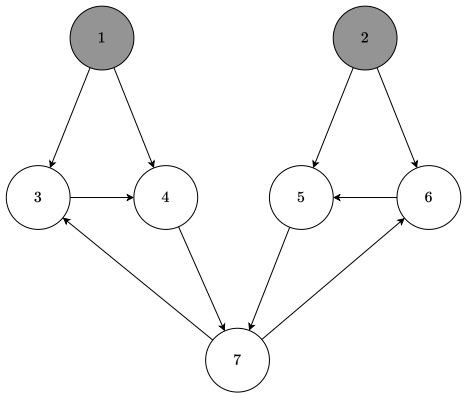

Fig. 4: Cyclical communication graph $\mathcal{G}_2$.

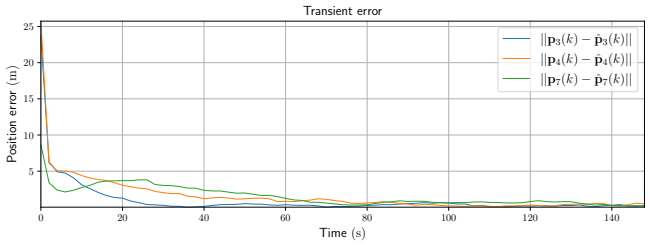

(a) CEKF position estimate error.

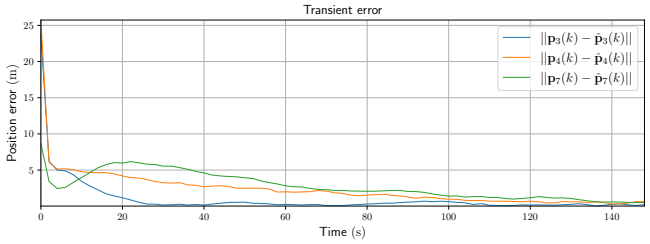

(b) DEKF position estimate error.

Fig. 5: Sample run position estimation errors.

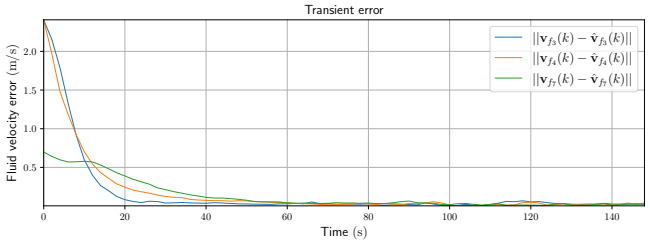

(a) CEKF fluid velocity estimate error.

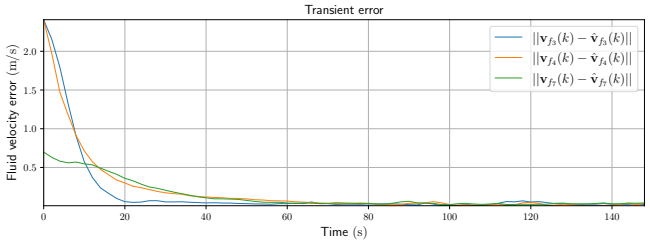

(b) DEKF fluid velocity estimate error.

Fig. 6: Sample run fluid velocity estimation errors.

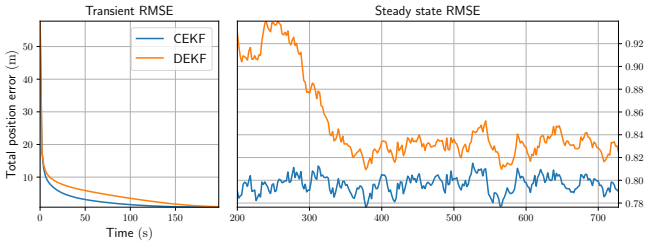

(a) Total position estimate RMSE.

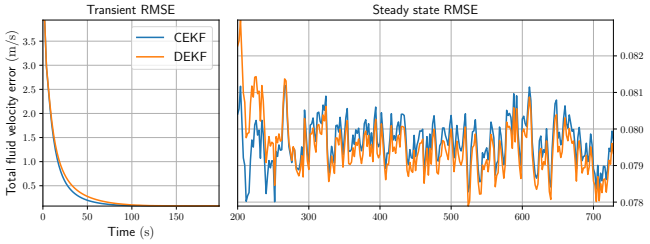

(b) Total fluid velocity estimate RMSE.

Fig. 7: Algorithm comparison for $\mathcal{G}_1$.

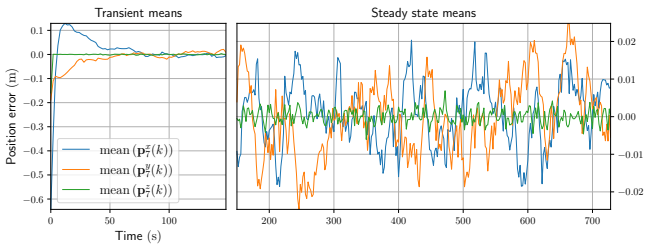

(a) CEKF mean position coordinate errors of AUV 7.

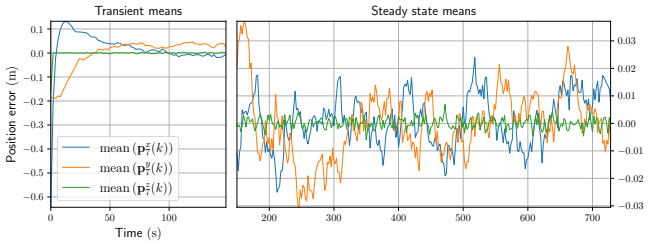

(b) DEKF mean position coordinate errors of AUV 7.

Fig. 8: Position coordinates means for $\mathcal{G}_1$.

behavior of the position and fluid velocity errors of both solutions for a sample run. As expected, the centralized filter converges to the solution faster than the DEKF, as the latter is missing measurement and cross-correlation information to other agents. However, the transient response was found to be heavily influenced by the initial conditions, with the DEKF sometimes outperforming the CEKF. In the following sections, Monte Carlo results are presented for the two topologies that were considered.

C. Acyclical communication graph results

Figs. 7a and 7b show the estimated position and fluid velocity RMSE for both algorithms, considering the acyclical communication topology, $\mathcal{G}_1$. As expected, the localization estimates provided by the CEKF are better than those computed by the decentralized algorithm. However, the fluid velocity estimates provided by the DEKF are slightly more accurate. This suggests that the filter was not correctly tuned, namely, that measurements were being given too much importance. However, because these are EKF-based approaches, if the estimates do not converge to the true solution fast enough, the filters might end up becoming overconfident and converging to non-optimal solutions or even diverge. In addition to the RMSE of the estimated quantities, the mean errors for the position coordinates of AUV 7 are also presented in Fig. 8, showing that both estimators are unbiased.

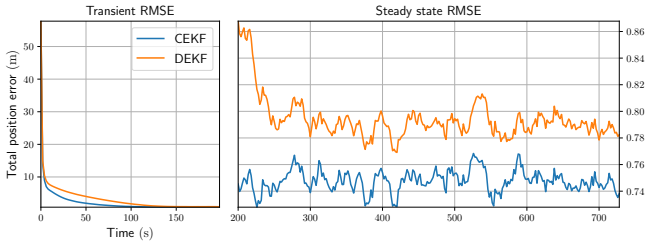

(a) Total position estimate RMSE.

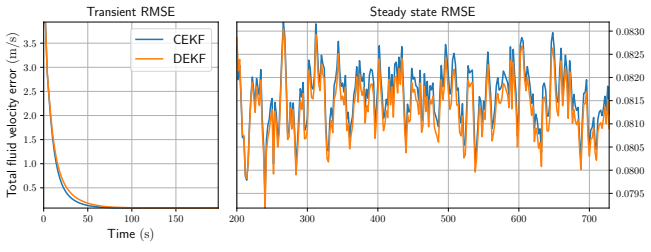

(b) Total fluid velocity estimate RMSE.

Fig. 9: Algorithm comparison for $\mathcal{G}_2$.

D. Cyclical communication graph results

Considering now the cyclical communication topology, represented by $\mathcal{G}_2$, the RMSE results for CEKF and DEKF are presented in Fig. 9. It is clear that, once again, the centralized estimator provides a better navigation estimate than the DEKF. And, once again, the DEKF's fluid velocity estimate is slightly better than CEKF's, due to the same reasons as before. Comparing the results presented in this section with those presented in the previous section, the position estimation has clearly benefited from the introduction of cycles. However, the fluid velocity estimate has degraded in both approaches due to the fact that there is more measurement information and too much importance had to be given to these to ensure convergence to the true solution. Regardless, the total estimation error is decreased upon the introduction of cycles, which, besides providing the formation with new measurement information, also increases the coupling between the agents, allowing for a more cooperative solution.

VI. Conclusion

In this work, two EKF-based approaches for the navigation problem of an AUV formation using depth and bearing measurements were analyzed via simulations and Monte Carlo results were presented. As expected, the centralized estimator provides better position estimates. Additionally, it was found that the presence of cycles allowed for more coupling between agents, which ends up being beneficial for both the convergence behavior of the estimators, as well as their steady-state position estimation performance. On the other hand, this was observed to be detrimental to the fluid velocity estimate of both solutions, which is due to the tuning balance that had to be performed because the approaches are EKF-based, and thus do not have global convergence guarantees. This emphasizes the clear benefits of observers with globally stable dynamics, which can be more easily tuned, and, unlike EKF-based approaches, have no need for relatively accurate initial state guesses, which would end up increasing the time efficiency of missions, since there is no need for an initial setup process.

Even though the CEKF provides a better localization estimate, it is often impractical to implement in a real system, especially for formations with many agents, due to its scalability problems. The DEKF is a simple, completely decentralized alternative, which provides navigation estimates similar to those of the CEKF and takes full advantage of the benefits that come with decentralization, such as scalability and robustness. Cycles improve the localization estimate of the system due to the increased coupling between agents, improving both the convergence and steady-state performance of the estimators, and, as such, should be exploited for more accurate localization estimates.

References

[1] S. S. Kia, S. Rounds, and S. Martinez, "Cooperative localization for mobile agents: A recursive decentralized algorithm based on kalman-filter decoupling," *IEEE Control Systems Magazine*, vol. 36, no. 2, pp. 86–101, 2016.

[2] L. Luft, T. Schubert, S. I. Roumeliotis, and W. Burgard, "Recursive decentralized localization for multi-robot systems with asynchronous pairwise communication," *The International Journal of Robotics Research*, vol. 37, no. 10, pp. 1152–1167, 2018.

[3] M. F. Fallon, G. Papadopoulos, and J. J. Leonard, "A measurement distribution framework for cooperative navigation using multiple auvs," in *2010 IEEE International Conference on Robotics and Automation*, pp. 4256–4263, IEEE, 2010.

[4] A. Bahr, M. R. Walter, and J. J. Leonard, "Consistent cooperative localization," in *2009 IEEE International Conference on Robotics and Automation*, pp. 3415–3422, IEEE, 2009.

[5] L. C. Carrillo-Arce, E. D. Nerurkar, J. L. Gordillo, and S. I. Roumeliotis, "Decentralized multi-robot cooperative localization using covariance intersection," in *2013 IEEE/RSJ International Conference on Intelligent Robots and Systems*, pp. 1412–1417, IEEE, 2013.

[6] A. Howard, M. J. Matark, and G. S. Sukhatme, "Localization for mobile robot teams using maximum likelihood estimation," in *IEEE/RSJ international conference on intelligent robots and systems*, vol. 1, pp. 434–439, IEEE, 2002.

[7] J. Zhang and H. Ji, "Distributed multi-sensor particle filter for bearings-only tracking," *International Journal of Electronics*, vol. 99, no. 2, pp. 239–254, 2012.

[8] D. Santos and P. Batista, "Decentralized navigation systems for bearing-based position and velocity estimation in tiered formations," in *2020 American Control Conference (ACC)*, pp. 5225–5230, IEEE, 2020.

[9] G. C. Calafiore, L. Carlone, and M. Wei, "A distributed technique for localization of agent formations from relative range measurements," *IEEE Transactions on Systems, Man, and Cybernetics-Part A: Systems and Humans*, vol. 42, no. 5, pp. 1065–1076, 2012.